

# Power Control Schemes for Land Mobile Satellite Communication Systems

Nam-Gil Lee, In-Tae Hwang, Seong-Hwan Kim, Cheol-Hun Na, and Sang-Jin Ryoo, *Member, KIMICS*

**Abstract**—In order to increase system capacity and reduce the transmitting power of the user's equipment, we propose an advanced power control scheme consisting of a modified open-loop power control (OLPC) and closed-loop power control (CLPC) for land mobile satellite communication systems. The improved CLPC scheme, combining delay compensation algorithms and pilot diversity, is mainly applied to the ancillary terrestrial component (ATC). ATC link in urban areas, because it is more suitable to the short round-trip delay (RTD).

**Index Terms**—power control, pilot diversity

## I. INTRODUCTION

IN 4G systems, the major role of satellites will be to provide terrestrial fill-in service and efficient multicasting/broadcasting services [1]. However, it is known that it is difficult for a mobile satellite service (MSS) to reliably serve densely populated areas, because satellite signals are blocked by high-rise structures and/or do not penetrate into buildings. Under these circumstances, in a groundbreaking application to the Federal Communication Commission (FCC) in 2001, Mobile Satellite Ventures LP (MSV) unveiled a bold new architecture for an MSS with an ATC providing unparalleled coverage and spectral efficiency [2]. The main concept of the hybrid MSS/ATC architecture of the MSV proposal is that terrestrial reuse of at least some of the satellite band service link frequencies can eliminate the above-mentioned problem. As the terrestrial fill-in services using ATC, satellite systems provide services and applications similar to those of terrestrial systems outside the terrestrial coverage area as much as possible. This paper

examines power control and handover using position information in land mobile satellite communication systems containing an ATC.

## II. POWER ESTIMATION AND PILOT DIVERSITY

Signal to interference plus noise ratio (SIR) estimation is one of the key aspects of the OLPC and CLPC scheme. SIR estimates are typically needed for functions such as power control, handoff, adaptive coding, and modulation. In this section, we focus on the third generation WCDMA FDD system and study the channel estimation in order to archive accurate energy of the desired signal [3][4].

The channel estimation using the pilot symbol structure periodically performs time-division multiplexing for data symbols and pilot symbols, which are known to a transmitter and a receiver, and transmits the multiplexed symbols. A channel change in a data symbol period is compensated with a channel estimation value in a pilot symbol period. The above channel estimation method is for estimating a channel using only the pilot symbols of a dedicated physical control channel (DPCCH). Another method compensates the data symbols for channel change by transferring pilot symbols, which are known to a transmitter and a receiver, using predetermined pilot symbol patterns. The above method estimates a channel using only a common pilot channel (CPICH). A disadvantage of the conventional channel estimation method is that it incurs more errors when a channel related to the channel estimation is under deep fading. It is, therefore, one of the objectives of our work to provide a channel estimation method with superior performance than channel estimation in a receiver of a terminal having conventional pilot symbols of a CPICH or a DPCCH. To this end, our method involves combining pilot symbols of a CPICH, a DPCCH, and a secondary common control physical channel (SCCPCH), and estimating a channel.

Efficient channel estimation is compared with a channel estimation method using only the pilot

Manuscript received January 3, 2009; revised March 1, 2009. Corresponding Author : Sang-Jin Ryoo is with the Dept. of Computer Media, Hanyeong College, Yeosu, 550-704, Korea (Tel : +82-61-650-4229, Email : sjryoo@empal.com, sjryoo@hanyeong.ac.kr)

symbols of the CPICH, as well as a channel estimation method combining the pilot symbols of the DPICH and those of the CPICH.

Eq.(1) represents a channel estimation using  $N$  symbols of the CPICH in one slot after a multipath fading and a despreading process in a RAKE receiver.

$$x(i) = \alpha(i) + n(i) \quad \text{for } i = 1, 2, \dots, N \quad (1)$$

in which  $N$  and  $\alpha(i)$  are the number of pilot symbols in one slot of the CPICH and a channel gain to be estimated, respectively, and  $n(i)$  is a noise including the interference of other cells, which assumes zero mean and  $\sigma_n^2$  variance. Eq.(2) shows a method for estimating a channel by combining the pilot symbols of the dedicated physical channel (DPCH) and pilot symbols of the CPICH. A receiver of a terminal acknowledges a pilot pattern for pilot symbols of the DPCH in a manner similar to Eq.(1).

$$y(j) = \lambda(j)\alpha(j) + m(j) \quad \text{for } j = 1, 2, \dots, M \quad (2)$$

in which  $M$  is the number of pilot symbols in one slot of the DPCH used in estimating a channel gain, and  $\lambda(j) = (1/\mu(j))^{1/2}$  refers to the power ratio of the pilot symbols of the DPCH and those of the CPICH. It is presumed that  $m(j)$  is an additive white Gaussian noise (AWGN) that has zero mean and  $\sigma_m^2$  variance. Since it is presumed that the channel gain is not changed during one slot of an estimation period,  $\alpha(i)$  and  $\lambda(i)$  become  $\alpha$  and  $\lambda$ , respectively. Eq.(3) shows a method for estimating a channel by combining the pilot symbols of the DPCH, those of the CPICH, and those of the S-CCPCH.

$$z(k) = \lambda_1(k)\alpha(k) + l(k) \quad \text{for } k = 1, 2, \dots, K \quad (3)$$

in which  $K$  is the number of pilot symbols in one slot of the S-CCPCH used in estimating a channel gain, and  $\lambda_1(k) = (1/\mu_1(k))^{1/2}$  refers to the power ratio of the pilot symbols of the S-CCPCH and those of the CPICH. It is presumed that  $l(k)$  is an AWGN that has zero mean and  $\sigma_k^2$  variance. Since it is presumed that the channel gain is not changed during one slot of an estimation period,  $\alpha(k)$  and  $\lambda_1(k)$  become  $\alpha$  and  $\lambda_1$ , respectively. Since channelization codes used in the CPICH, the DPCH, and the S-CCPCH are different from each other,  $n(i)$ ,  $m(j)$ , and  $l(k)$  are independent of each other. It is possible to perform the above processes, although the channels overlap at the same time. A vector of a signal received in a rake receiver of a terminal is as follows:

$$z' = [x(1)x(2)\cdots x(N)y(1)y(2)\cdots y(M)z(1)z(2)\cdots z(L)]^T \quad (4)$$

where  $T$  denotes an operator of a transpose matrix. If  $\lambda$ ,  $\lambda_1$ , and  $\alpha$  are known, a conditional probability density function is as follows:

$$p(z|\lambda_1, \lambda, \alpha) = \left( \frac{1}{\sqrt{2\pi\sigma_n^2}} \right)^N \left( \frac{1}{\sqrt{2\pi\sigma_m^2}} \right)^M \left( \frac{1}{\sqrt{2\pi\sigma_k^2}} \right)^K \quad (5)$$

$$\times \exp \left( -\sum_{i=1}^N \frac{(x(i) - \alpha)^2}{2\sigma_n^2} - \sum_{j=1}^M \frac{(y(j) - \lambda\alpha)^2}{2\sigma_m^2} - \sum_{k=1}^K \frac{(z(k) - \lambda_1\lambda\alpha)^2}{2\sigma_k^2} \right)$$

where  $\alpha$  denotes a channel estimation value (case 1) using the CPICH,  $\lambda$  denotes a channel estimation value (case 2) combining the DPCH and the CPICH [5][6], and  $\lambda_1$  denotes a channel estimation value (case 3) combining the CPICH, the DPCH, and the S-CCPCH. A Cramer-Rao Lower Bound (CRLB) is used to analyze the performances of the above cases to compare channel estimation values of the above cases. Then, a performance analysis is performed, as follows, by comparing case 2 with case 3 through the use of a Fisher information matrix. Subsequently, case 2 is compared with case 3, as described in Eq.(6), by using the aforementioned CRLB, to show that the performance of the developed method is superior to those of the other methods through the use of the Fisher information matrix.

$$I(\lambda_1, \alpha) = \begin{bmatrix} -E \left( \frac{\partial^2 \ln p(z|\lambda_1, \lambda, \alpha)}{\partial^2 \lambda_1} \right) & -E \left( \frac{\partial^2 \ln p(z|\lambda_1, \lambda, \alpha)}{\partial \lambda_1 \partial \alpha} \right) \\ -E \left( \frac{\partial^2 \ln p(z|\lambda_1, \lambda, \alpha)}{\partial \alpha \partial \lambda_1} \right) & -E \left( \frac{\partial^2 \ln p(z|\lambda_1, \lambda, \alpha)}{\partial^2 \alpha} \right) \end{bmatrix} \quad (6)$$

$$= \begin{bmatrix} \frac{K\lambda^2\alpha^2}{\sigma_k^2} & \frac{2\lambda_1\lambda^2\alpha K}{\sigma_k^2} \\ \frac{2\lambda_1\lambda^2\alpha K}{\sigma_k^2} & \frac{N}{\sigma_n^2} + \frac{M\lambda^2}{\sigma_m^2} + \frac{K\lambda_1^2\lambda^2}{\sigma_k^2} \end{bmatrix}$$

If  $\lambda_1$  is known, the output CRLB is that shown by Eq.(7).

$$CRLB(\hat{\alpha}|\lambda_1) = \frac{1}{I(\lambda_1, \alpha)_{2,2}} = \frac{1}{\frac{N}{\sigma_n^2} + \frac{M}{\mu\sigma_m^2} + \frac{K}{\mu\mu_1\sigma_k^2}} \quad (7)$$

Accordingly, comparing [7] with Eq.(7) results in Eq.(8), as follows.

$$\frac{1}{\frac{N}{\sigma_n^2} + \frac{M}{\mu\sigma_m^2} + \frac{K}{\mu\mu_1\sigma_k^2}} \leq \frac{1}{\frac{N}{\sigma_n^2} + \frac{M\lambda^2}{\sigma_m^2}} \leq \frac{\sigma_n^2}{N} \quad (8)$$

As a result, it can be seen that the channel estimation combining the CPICH, the DPCH, and the S-CCPCH is superior to both the channel estimation using only the CPICH and the channel estimation combining the CPICH and the DPCH.

### III. OPEN-LOOP AND CLOSED-LOOP POWER CONTROL

#### A. Open-loop Power Control

Conventionally, uplink and downlink power control may be based on a combination of open- and/or closed-loop methods. A modified OLPC and CLPC model is shown in Fig. 1. In the OLPC, the UE estimates a transmitting power level, which may maintain a desired signal quality and/or strength at a base transceiver system (BTS) or base station, by monitoring its own received quality. In other words, the mobile's transmitting power is determined by measuring the received signal strength of the base station and estimating the forward link path loss. Assuming a similar path loss for the reverse link, the mobile unit uses this information to determine its transmitter power. In the IS-95 system reverse link, power control is used to compensate for the signal power fluctuation at the base station due to path loss and shadowing, as well as small-scale fading. This technique is crucial to the system performance, due to its role in preventing a near-far effect and in mitigating fading. The OLPC adjusts the transmitted signal power level according to the received forward link signal strength. Hence, it mainly compensates for path loss and shadowing, while the CLPC is designed to compensate for the small-scale fading caused by the multipath in the transmission on the reverse link, which is different from that on the forward link, due to the frequency separation of the links. As mentioned in Section III, in order to improve the accuracy of the estimation of SIR, we proposed a method to estimate the interference power, which will be presented as follows.

In Fig. 2,  $n$ ,  $k$ ,  $l$ ,  $T_b$ , and  $T_c$  denote  $n$ -th slot,  $k$ -th symbol,  $l$ -th resolvable multi-path, bit duration, and chip duration, respectively. In addition,  $SIR_{DPCH}(n,k,l)$ ,  $SIR_{CPICH}(n,k,l)$ , and  $SIR_{SCCPCH}(n,k,l)$  stand for estimates of CPICH, S-CCPCH, and DPCH, respectively. SIR is an important power control system parameter that has a profound effect on system

capacity as the desired signal and the interference have the same bandwidth at the output of the digitally matched filter, SIR. Since the interference noise is Gaussian distributed, the variance of the interference can be found from the sum of the variances of the amplitude of the  $I$  channel and  $Q$  channel, as follows:

$$I = E|R_I|^2 + E|R_Q|^2 \quad (9)$$

Desired signal  $S$  is achieved by calculating the summation of the  $S_l$  from the 1 to  $L$  tap RAKE receiver.

$$S = \sum_{l=0}^{L-1} S_l \quad (10)$$

According to Friis' free-space propagation-path-loss formula [8], in order to apply OLPC, the average received power at the mobile station would be:

$$P_r = |E|^2/2\eta_0 = P_0[1/(4\pi d/\lambda)]^2 \quad (11)$$

where  $P_0 = P_t G_t G_m$  and  $\eta_0$ ,  $P_t$ ,  $G_t$ , and  $G_m$  denote intrinsic impedance of free-space, transmitted power, gain of the transmitting antenna, and gain of the receiving antenna, respectively.

Path loss and shadowing effects are regarded as slow fading in this work. To compensate for slow fading, the CDMA 2000 system has defined a standard equation for the mobile station to perform OLPC for the air interface in [9]. The general open-loop response of the OLPC can be approximated as follows [10]:

$$O(t) = -\Delta P_{in}(1-\exp(-t/\tau))u(t) \quad (12)$$

In Eq.(12),  $\Delta P_{in}$ ,  $\tau$ , and  $O(t)$  are the step change in mean input power, the time constant of the open-loop response, and the output. The OLPC output response of UE serving from ATC is close to that specified in the standards if  $\tau$  is 20 ms. We assume that the operation period of the OLPC output response of UE serving from a GEO satellite is 250 ms. In this paper, it is added to the monitoring equipment in OLPC to use information about the transmitting power that has not yet been received by the receiver over the satellite/ATC channel.

#### B. Closed-loop Power Control

CLPC is a powerful tool to mitigate near-far problems in a direct-sequence code division multiple access (DS-CDMA) system over Rayleigh fading channels [11]. The SAT/ATC advises the UE of

adjustments to the transmitting power level that may have initially been set by the OLPC. This form of power control (open- and/or closed-loop) may increase the UE's EIRP to the maximum in order to maintain link connectivity and/or acceptable link quality. Because of a significant difference in the RTD, there is serious performance degradation of the CLPC if the power control used for the terrestrial interface is employed as is. In order to reduce power control error, a delay compensation mechanism was selected in the ATC and satellite.

For the case of the uplink CLPC, the UE calculates the actual amount of the transmission power control by using the two most recently received power control commands, which are aimed to change the loop dynamics and shorten the latency in updating the transmission power. For the case of the downlink CLPC, the UE may employ a prediction algorithm that estimates the future SIR value after an RTD by observing the SIR of the CPICH and S-CCPCH. The power control command is generated on the basis of the predicted SIR value. The RTD of a GEO system results in significant performance degradation of the CLPC if the 3GPP standard is employed as is [12]. There are two main problems that degrade the CLPC under such a long RTD. The first problem is instability in the internal loop dynamics, because the power control step size specified in 3GPP is too large to keep the loop stable under such a long loop delay. In other words, the measurements at the UE do not reflect the results of the most recent power updates at the satellite radio access network (S-RAN) and ATC network. The second problem is the possibility of a large number of SIR changes during the loop delay, resulting in a large power control error. As an effective solution to the first problem, Gunnarsson proposed a delay compensation power control scheme [13], and this was reflected in the S-UMTS standard [14]. Although this can effectively cancel the internal RTD in the power control loop, the second problem remains.

In order to solve the second problem, we proposed a prediction algorithm that estimates the future SIR value after an RTD. We now present our proposed algorithm in more detail by focusing on the downlink CLPC scheme. We apply it to a GEO system, and will demonstrate delay compensation performance. The power control adjusts the S/ATC-RAN transmitting power in order to keep the received downlink power SIR at a given SIR target,  $SIR_{target}$ . The UE estimates the SIR of the received downlink DPCCCH and the SIR variation of the received CPICH and S-CCPCH, where the CPICH channel and the S-CCPCH are not power

controlled and are power controlled, respectively, then generates two-bit transmitting power control (TPC) commands every 10 ms (per frame) [15]. The TPC commands are generated as follows. Firstly, let us define power control error of  $\Delta_{e,c} = SIR_{est} - SIR_{target} + \Delta_{loop\ delay}$ , where  $\Delta_{loop\ delay}$  and  $SIR_{est}$  denote the prediction for the amount of SIR increment/decrement of the received downlink CPICH, S-CCPCH, and the estimated SIR of the received downlink DPCCCH during the next time interval equal to the loop delay, respectively. Therefore,  $\Delta_{loop\ delay}$  is added to  $SIR_{est}$  to result in the predicted SIR value of  $SIR_{est,pred}$ . In other words, we employed a simple algorithm to calculate  $\Delta_{loop\ delay}$  as follows:

$$\Delta_{loop\ delay} = n \times \Delta_{pred} \quad (13)$$

where  $n \times \Delta_{pred}$  is the increment (or decrement) of the estimated SIR of CPICH and S-CCPCH in dB during the last frame, and  $n$  is the nearest integer to (loop delay)/(frame length). A four-level quantized power control step,  $\Delta_p$ , is generated according to the region of  $\Delta$ , as follows:

$$\begin{aligned} \text{if } |\Delta_{e,c}| < \varepsilon_T \text{ and } \Delta_{e,c} < 0, \quad \Delta_p(i) &= \Delta_S \\ \text{if } |\Delta_{e,c}| < \varepsilon_T \text{ and } \Delta_{e,c} > 0, \quad \Delta_p(i) &= -\Delta_S \\ \text{if } |\Delta_{e,c}| > \varepsilon_T \text{ and } \Delta_{e,c} < 0, \quad \Delta_p(i) &= \Delta_L \\ \text{if } |\Delta_{e,c}| > \varepsilon_T \text{ and } \Delta_{e,c} > 0, \quad \Delta_p(i) &= -\Delta_L. \end{aligned}$$

In the statements above,  $\Delta_S$ ,  $\Delta_L$ , and  $\varepsilon_T$  are a small power control step, a large power control step, and the error threshold, respectively. Because of the RTD in the GEO system, the S-RAN can reflect  $\Delta_p(i)$  at its transmission power after about 250 ms, during which time there may be a considerable change in the SIR. We employ a simple preprocessing for  $\Delta_p(i)$  before it is reflected at the transmission power in order to compensate for the RTD. The S-RAN adjusts the transmitting power of the downlink DPCCCH with an amount of DPCCCH using the two most recently received power control steps,  $\Delta_p(i)$  and  $\Delta_p(i-1)$ , and this can be modeled as a simple finite impulse response filter (FIR), as follows [16]:

$$\begin{aligned} \Delta_{DPCCCH} &= \Delta_p(i) - \alpha \Delta_p(i-1) \\ &= (1-\alpha)\Delta_p(i) + \alpha(\Delta_p(i) - \Delta_p(i-1)) \end{aligned} \quad (14)$$

which means that  $\Delta_{DPCCCH}$  is determined not only by  $\Delta_p(i)$  but also by the difference between  $\Delta_p(i)$  and  $\Delta_p(i-1)$  with weighting factors of  $(1-\alpha)$  and  $\alpha$ , respectively. As  $\alpha$  increases,  $\Delta_{DPCCCH}$  becomes more dependent upon the term  $\Delta_p(i) - \Delta_p(i-1)$ , which corresponds to an

estimate for the amount of the recent channel variation.

#### IV. SIMULATION RESULTS

A channel with only fast fading and a channel with path loss, slow fading, and fast fading were simulated to examine the performance of the CLPC with and without an OLPC. The simulation parameters are given in table 1. We present the simulation results of only the proposed CLPC scheme (SCHEME-II), combining the proposed OLPC and proposed CLPC (SCHEME-I), and only the proposed OLPC (SCHEME-III) over GEO satellite or ATC environments, and we compare the performance of the various conventional- OLPC and CLPC algorithms. For conventional schemes, we used the terrestrial CLPC scheme in the WCDMA system and Gunnarsson's scheme in [15], and they are denoted in the figures as SCHEME-II with a dotted line and without SCHEME-II with a dotted line. For reference, the part shown as the dotted line and solid line means without pilot diversity and with pilot diversity, respectively. In our simulations, we consider a satellite system with a single beam and ignore the inter-spot interference. We assume that the path loss exponent is taken to be 2. For the simulations, we chose a target SIR of 5dB. We selected a processing gain (PG) of 256. We assumed power control begins to work after 250ms due to propagation delay.

Assuming the same parameters for the channel and a mobile speed of 98km/h, performance of our system and the other system with increased power control command error probability is illustrated in figures 3 and 4. As shown in the figures, the combined proposed OLPC and CLPC (SCHEME-I shown in solid line) is also still powerful compared to other system. This algorithm efficiently removes the shadowing effect and simultaneous slow/fast fading of the UE serving from the GEO satellite. For the UE serving from ATC, the power control error of SCHEME-I using pilot diversity is superior to the other scheme when the normalized Doppler frequency of the UE is zero because of power estimation when using pilot diversity. However it is seen that at low vehicle speeds (14~42km/h), performance of SCHEME-I and II which is monitoring transmitting power is inferior to other schemes because conventional CLPC is an insensitive short RTD. We note in Fig. 3 that the standard deviations in the power control error of SCHEME-I with pilot diversity, SCHEME-II with pilot diversity, SCHEME-I without pilot diversity, and SCHEME-II without pilot diversity were 1.0156dB, 1.0157dB, 1.024dB, and 1.023dB,

respectively, when mobile speed was 70km/h. There was a decrease in the standard deviation of errors in SIR for the scheme with the pilot diversity compared with the other scheme. We also observed that the increase in the standard deviation due to combining monitoring transmitting power and the OLPC scheme became relatively smaller as the mobile speed increased from 0km/h to 96km/h.

Figures 3 and 4 illustrate power control error according to mobile speed. When employing our efficient pilot diversity and monitoring equipment of power control scheme, power control shows greater stability, which is important in the sense of the network. From the figures, we observe that the standard deviation of the power control error in SIR increased as the mobile speed increased. In Fig. 4, for SCHEME-I using pilot diversity, the standard deviation of the power control error in SIR was 1.59dB for a mobile speed of 56km/h, while that in SCHEME-II using pilot diversity was approximately 1.65dB for a mobile speed of 56km/h. The combining of monitoring transmitting power and OLPC scheme in SCHEME-I using pilot diversity efficiently removed path loss and slow fading, because if fast fading can be approximately tracked, then there is little difficulty in coping with much slower variations in path loss and slow fading.

Figures 5 and 6 show the probability density function of the received SIRs for a mobile speed of 98km/h having a probability of power control command error of 0. Intuitively, we turn out that the SCHEME-I using pilot diversity has a larger improvement, as confirmed in the simulation results. As we can see, the powers of the user in the case described in Fig. 6 with SCHEME-I using pilot diversity converge to the target SIR of 5dB. On the other hand, those of the other schemes result in a higher SIR estimation error.

#### V. CONCLUSIONS

Conventional channel estimation methods incur many errors in the case of deep fading. In contrast, the proposed channel estimation method using the S-CCPCH to the conventional methods can obtain an improved pilot diversity gain by performing channel estimation using other channels when the first channel does not reach a required level of a received signal. Thus, it is possible to implement an ideal maximum ratio combining method in a RAKE receiver. The channel estimation method described in this paper provides a more improved performance than channel estimation in a receiver of a

terminal having conventional pilot symbols of a CPICH or a DPCCH by combining pilot symbols of a CPICH, a DPCCH, and a S-CCPCH, and estimating a channel. In this paper, we have presented satellite access technologies for a future mobile system. We suggested desirable modifications for application to the 4G system. Combining modified CLPC and OLPC with delay compensation algorithms and monitoring equipment proved to provide a good performance in a MSS/ATC hybrid system. In addition, to increase the performance and to keep commonalities between terrestrial standards, more advanced transmission technologies, including multi-carrier transmission, interference cancellation, and highly efficient modulation and coding should be investigated in more detail.

## REFERENCES

- [1] "Estimates of MSS subscriber numbers and traffic profiles for the ASMS-TF," ESYS Consulting, 2003.
- [2] I. Philipopoulos, S. Panagiotarakis, and A. Yanelli-Coralli, "The role of S-UMTS in future 3G markets," IST-2000-25030 SATIN Project, SUMTS.P-specific requirement, deliverable No. 2, April 2002.
- [3] D. Pauluzzi and N. Beaulieu, "A Comparison of SNR estimation techniques for the AWGN channel," IEEE Trans. On Commun., vol. 48, no. 10, pp. 1681-1691, Oct. 2000.
- [4] S. Seo et al "SIR-Based transmit power control of reverse link for coherent DS-CDMA mobile radio," IEICE Trans. Commun., vol, E81-B, no. 7, pp. 1508-1516, July 1998.
- [5] T. Luo and Y. C. Ko, "Pilot diversity channel estimation in power-controlled CDMA systems," IEEE Trans. On Veh. Tech., vol. 53, no. 2, pp. 559-563, Mar. 2004.
- [6] M. Usuda, Y. Ishikawa, and S. Onoe, "Optimizing the number fo dedicated pilot symbols for forward link in WCDMA systems," in Proc. IEEE VTC'00, pp. 2118-2122, June 2000.
- [7] H. V. Khuong, and H. Y. Kong, "BER Performance of cooperative transmission for the uplink of TDD-CDMA systems," ETRI Journal, vol. 28, no. 1, pp. 17-30, Feb. 2006.
- [8] C. -C. LEE, and R. Steele, "Closed-loop power control in CDMA systems," IEE Proc. Comm., vol.143, no.4, pp.231-239, Aug. 1996.
- [9] 3GPP2 TSG-C, "Physical Layer Standard for cdma2000 spread spectrum systems – Release 0," May 2001.
- [10] S. Choe, "An analytical framework for imperfect DS-CDMA closed-loop power control over flat fading," ETRI Journal, vol. 27, no. 6, pp. 810-813, Dec. 2005.

- [11] T. Chulajata, and H. M. Kwon, "Combinations of power controls for cdma2000 wireless communications system," in Proc. IEEE VTC2000, vol. 2, pp. 638-645, Sept. 2000.
- [12] 3GPP TS 25.214, "Physical layer – Procedures (FDD) – Release 5," 2004.
- [13] F. Gunnarsson, and F. Gustafsson, "Time delay compensation in power controlled cellular radio systems," in IEEE Commun. Letter, vol. 5, no. 7, pp. 295-297, July 2001.
- [14] ETSI TS 101 851-4 "Satellite component of UMTS/IMT2000: A-family: Part 4, Physical layer procedures (S-UMTS-A 25.214," Nov. 2000.
- [15] Recommendation ITU-R M.1457, "Detailed specifications of radio interfaces of IMT-2000," 2001.
- [16] K. Lim, K. Choi, K. Kang, S. Kim, and H. J. Lee, "A satellite radio interface for IMT-2000," ETRI Journal, vol. 24, no. 6, pp. 415-428, Dec. 2002.

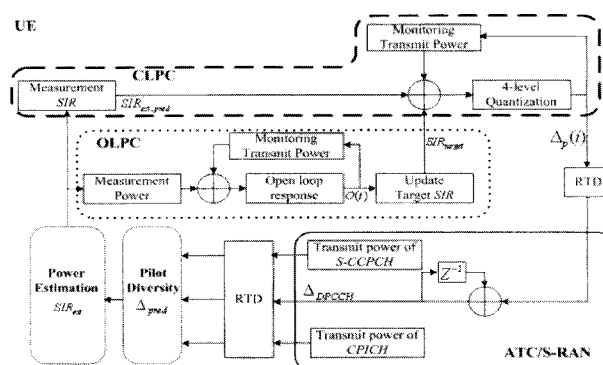


Fig. 1 Modified OLPC and CLPC model.

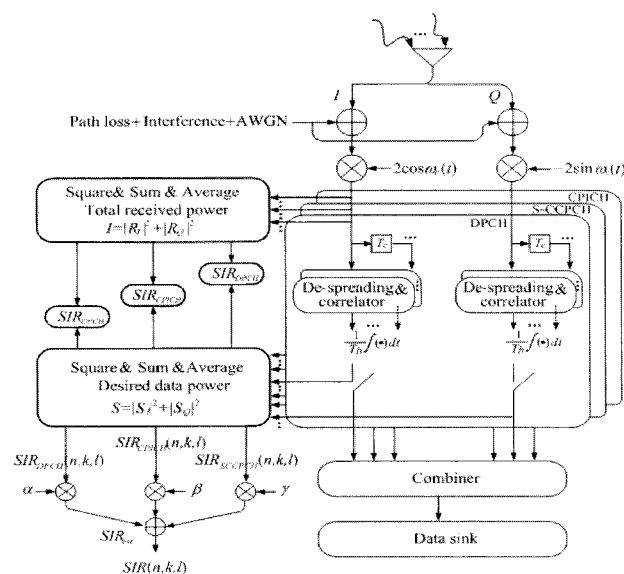


Fig. 2 Block diagram of power estimation using pilot diversity.

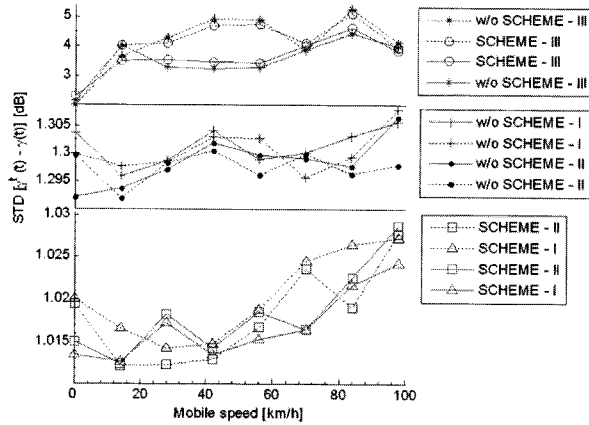


Fig. 3 Control error UE serving from ATC: standard deviation of target SIR minus received SIR according to mobile velocity.

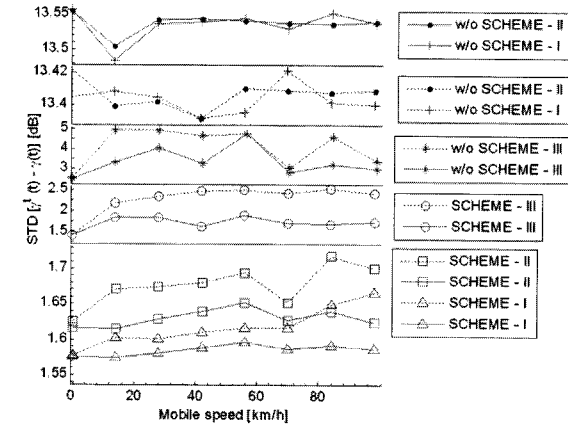


Fig. 4 Control error UE serving from GEO satellite: standard deviation of target SIR minus received SIR according to mobile velocity.

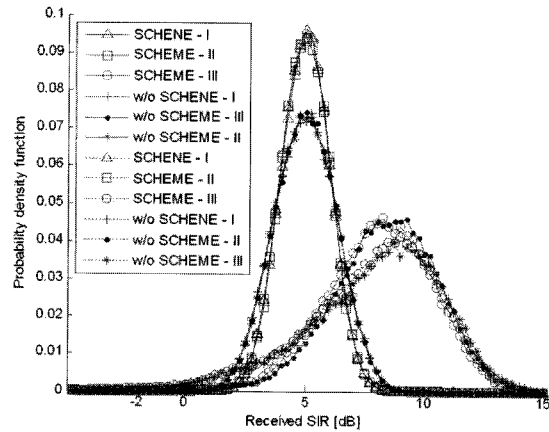


Fig. 5 Probability density function of received SIRs of UE serving from ATC:  $K = -\infty$  and  $V = 98 \text{ km/h}$ .

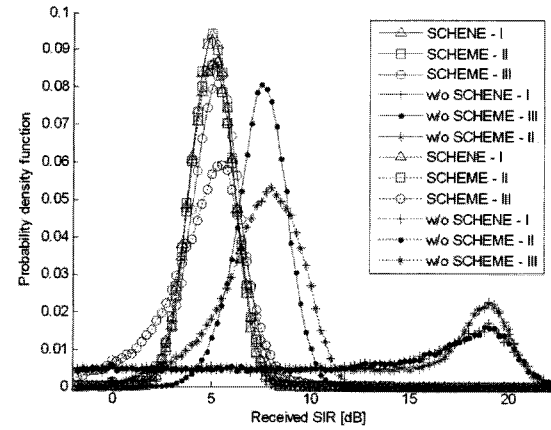
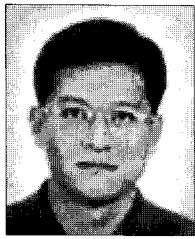


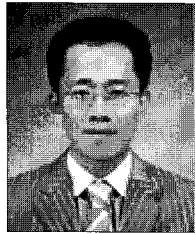
Fig. 6 Probability density function of received SIRs of UE serving from GEO satellite:  $K = 5 \text{ dB}$  and  $V = 98 \text{ km/h}$ .

Table 1 Simulation environment

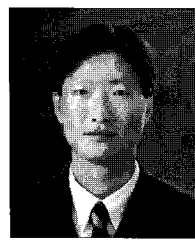
Parameter	Value	
Carrier frequency ( $f_c$ )	2170 MHz	
Power control sample interval ( $T_d$ )	UE serving from GEO satellite	10 ms
	UE serving from ATC	6.667E-4 ms
Frame length	10 ms	
Round trip delay	GEO satellite	250 ms
	ATC	< slot duration ( $\approx 6.667\text{E-}4 \text{ ms}$ )
Processing gain	256 ( $\approx 24 \text{ dB}$ )	
Transmit frame	UE serving from GEO satellite	70,000 frames
	UE serving from ATC	60,000 slots
Small step size	1 dB	
Large step size	2 dB	
Fading model	Clarke's model	
Target SIR	5 dB	
Desired received power	-140 dBW ( $\approx -110 \text{ dBm}$ )	
Rician K-factor	UE serving from GEO satellite	5 dB
	UE serving from ATC	$-\infty$
Power command error probability	0 ~ 0.15	
Interference plus noise power	-123 dBm	
Interference variance	6 dB	
Path loss variance	8 dB	
Maximum transmitting power	GEO satellite	41.8 dBW
	ATC	28 dBm
Minimum transmitting power	GEO satellite	-2.9 dBW
	ATC	-61 dBm
Mobile speed	0 ~ 98 km/h	



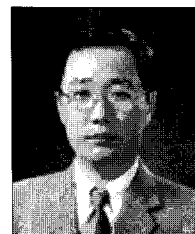
**Nam-Gil Lee** received the B.S., M.S. degrees in electronics engineering from Chonnam University, Kwangju, Korea, in 1992, 1996, respectively. Since February 1997, he has been with the Department of Information & Communication System, Korea Polytechnic College, Korea. He is currently interested in Information & Communication Network Systems.



**In-Tae Hwang** received the B.S. degree in Electronics Engineering from Chonnam National University, Gwangju, Korea in 1990 and the M.S. degree in Electronics Engineering from Yonsei University, Seoul, Korea in 1992, respectively and the Ph.D. degree in Electrical & Electronics Engineering from Yonsei University, Seoul, Korea in 2004. He had been as a senior engineer at LG Electronics from 1992 to 2005. He is currently in Chonnam National University, Gwangju, Korea from 2006 as a Professor in the School of Electronics & Computer Engineering. His current research activities are in digital & wireless communication systems, mobile terminal system for next generation, and efficient algorithms for AMC, MIMO and MIMO-OFDM.



**Seong-Hwan Kim** received the B.S., M.S., and Ph.D in Electrical Engineering from Korea University, Seoul, Korea in 1991, 1995 and 1998 respectively. He is an Associate Professor in the Department of Control System Engineering, Mokpo National University, Korea. His main research interests are the application of intelligent control to ac motor drivers and power electronics.



**Cheol-Hun Na** received the B.S., M.S., and Ph.D. Degree from Electrical Engineering, Chonnam National University in 1985, 1987, and 1994, respectively. From 1995, he worked as a professor of Mokpo National University. His research interest is in the area of Digital Image Processing, and Communication Engineering.



**Sang-Jin Ryoo** received the B.S., M.S., and Ph.D. degrees in electronics engineering from Chonnam University, Kwangju, Korea, in 1991, 1994, and 2007, respectively. Since March 1994, he has been with the Department of Computer Media, Hanyeong College, Yeosu, Korea. This author became a Member of IEICE in 2007. He is currently interested in mobile communication, channel coding, AMC, MIMO, and MIMO-OFDM systems.